
DEEP MOMENT MATCHING KERNEL FOR MULTI-SOURCE GAUSSIAN PROCESSES

A PREPRINT

Chi-Ken Lu

Department of Mathematics & Computer Science
Rutgers University Newark
New Jersey 07102
CL1178@rutgers.edu

Patrick Shafto

Department of Mathematics & Computer Science
Rutgers University Newark
New Jersey 07102
patrick.shafto@rutgers.edu

September 4, 2022

ABSTRACT

Human learners have the ability to solve new tasks efficiently if previous knowledge is relevant, which has motivated research into few-shot learning and transfer learning. We formalize the integration of relevant knowledge as multi-source regression in which the target function is inferred using Gaussian Process (GP) with the deep moment matching (DMM) kernel. We obtain a non-stationary DMM kernel from prior relevant data by analytically calculating the covariance of the target function. We interpret the data-informed DMM kernel, which serves as prior for target function, as: (1) a refined similarity determined by squared distance in the latent space and (2) as propagating uncertainty measured in RKHS defined by the posterior covariance from the prior learning. In comparison with the autoregressive models, variational DGP models and others, results show GP regression with the DMM kernels is effective when applying to the standard synthetic and real-world multi-fidelity data sets.

1 Introduction

A Gaussian Process (GP) (Rasmussen and Williams, 2006) is a collection of indexed random variables whose joint and marginal distributions are Gaussian, characterized by mean $\mu(\mathbf{x})$ and covariance $k(\mathbf{x}, \mathbf{x}')$ functions. In Bayesian regression, GP along with the selected covariance function shapes the hypothesis space where the true function $y = f(\mathbf{x})$ is believed to reside. For example, GP with squared exponential (SE) covariance function is suitable as a prior for domains explained by smooth functions, but not for domains where one may need to explain abrupt changes, e.g. step functions. Practitioners often manually select or design kernels to capture the structure of their domain of interest. In contrast with this manual and data intensive process, human learners are able to automatically leverage previous relevant experience to adapt hypothesis spaces that can recognize patterns and predict outcomes in new domains based on limited observations.

Deep models for regression tasks allow expressiveness about the possible patterns in a domain, but require large amounts of data from the target domain to train and inference is challenging. For example, deep kernels in Wilson et al. (2016) are built on the expressive power of neural network mapping h so that the kernel $k(h(\mathbf{x}), h(\mathbf{x}'))$ can be optimized to capture the varying length scales and signal magnitudes at different locations. Such compositional structure is common in deep probabilistic models as well. Deep Gaussian Process (DGP) (Damianou and Lawrence, 2013) with S -layers are comprised of S conditional GPs connected in a nested structure by which composition of functions $f \circ h^{(S-1)} \circ \dots \circ h^{(1)}(\mathbf{x})$ is modeled. Each individual GP in DGP allows arbitrary mean and covariance functions, which gives rise to a rich prior functional space that can be interpreted as kernel composition. However, the expressive power of DGP comes with a cost of intractable inference as the marginalization of intermediate functions, $h^{(1:S-1)}$, which is typically approximated via inducing points in variational settings (Damianou and Lawrence, 2013; Bui et al., 2016; Salimbeni and Deisenroth, 2017).

In this paper, we combine the advantages of multiple sources of data with expressiveness of deep GP and analytically tractable, interpretable approximate inference via moment matching, to provide a novel approach to prediction based on limited data. In the context of multi-source regression, we are given $S > 1$ data sets: the *target* data set, $\mathcal{D}_T = \{\mathbf{X}, \mathbf{y}\}$, and the *relevant* data sets, $\mathcal{D}_R = \{\mathbf{X}^{(i)}, \mathbf{y}^{(i)}\}_{i=1}^{S-1}$. One may consider \mathcal{D}_T as observations of the target function, while \mathcal{D}_R are observations of another function from a related domain. Here, we assume that the target and relevant observations satisfy some mapping, i.e. $y^{(t)} = f(\mathbf{x}, h(\mathbf{x})) = f(\mathbf{x}, y^{(r)})$, which allows us to cast the problem in DGP structure (Cutajar et al., 2019a). For each source in \mathcal{D}_R each datum $(\mathbf{x}^{(i)}, y^{(i)})$ is instance of the latent mapping $h^{(i)} \circ \dots \circ h^{(1)}$. Consequently, the GPs in intermediate layers represent the constrained space of functions which realize \mathcal{D}_R . In the absence of \mathcal{D}_T , this can be considered as an expressive prior distribution for the target function inferred from a related domain.

To ensure interpretability, we approximate intractable Bayesian inference via an analytic approximation. We focus on the second moment, the covariance, of the DGP marginal distribution in which the latent mappings are integrated exactly. Unlike the variational approach where all hidden mappings are inferred from an approximate DGP posterior distribution augmented with inducing points, we obtain the effective deep kernel by moment matching, which allows us to analytically study the origin of expressive power of DGP (Lu et al., 2020). Moreover, the target regression is tackled analytically with a single GP and the DMM kernel which retains the covariance of DGP. This is in contrast to the prediction stage in variational method where expensive Monte Carlo sampling from approximate posterior is required (Salimbeni and Deisenroth, 2017; Cutajar et al., 2019a).

In Sec. 1.1, we highlight novel mathematical properties of DMM kernels as approximation to the deep regression model for learning from relevant data. In Sec. 1.2, relevant works on deep probabilistic models, deep kernels, and approximate inference are discussed. In Sec. 2 and 3, notation and analytical calculations of target covariance are introduced. In Sec. 4 simulation results on standard synthetic and real-world data are presented, and Sec. 5 presents conclusions.

1.1 Why DMM kernel?

The Deep Moment Matching (DMM) kernel allows representation of relevant knowledge from \mathcal{D}_R in the form of analytic kernel without encountering the inverse of covariance matrix. Thus, we can calculate the covariance of the target function directly. This allows analytic construction of a prior on functions for \mathcal{D}_T from \mathcal{D}_R .

Table 1: Essential form of deep kernels

Kernel	Essential form
Deep kernel (Wilson et al., 2016)	$e^{-d_{\mathbf{h}}(\mathbf{x}, \mathbf{y})}$
DGP kernel (Duvenaud et al., 2014)	$e^{-d_k(\mathbf{x}, \mathbf{y})}$
NARGP (Perdikaris et al., 2017)	$e^{-d_{\mu}(\mathbf{x}, \mathbf{y})}$
DMM kernel	$e^{-d_{\mu}(\mathbf{x}, \mathbf{y})} / \mathcal{L}_{\mathbf{x}, \mathbf{y}}$

Additionally, DMM kernels have desirable properties for multi-source learning as compared with other deep kernels. In Table 1, we list a few deep kernels relevant to the discussion. Note that we neglect the corresponding hyper-parameters and focus on the most essential form.

The deep kernel in Wilson et al. (2016) models the covariance in composite function $f(\mathbf{h}(\mathbf{x}))$ with deterministic mapping \mathbf{h} by generalizing the SE kernel and replacing the squared Euclidean distance in input space with the distance $d_{\mathbf{h}}(\mathbf{x}, \mathbf{y}) = |\mathbf{h}(\mathbf{x}) - \mathbf{h}(\mathbf{y})|^2$ in the feature space.

When the latent mapping \mathbf{h} is of probabilistic nature, the DGP kernel in Duvenaud et al. (2014) shows the squared distance in RKHS (Schölkopf et al., 1998) as a signature of a kind of marginalization over \mathbf{h} . The squared distance in RKHS, i.e between $k(\mathbf{x}, \cdot)$ and $k(\mathbf{y}, \cdot)$, is exactly $d_k = k(\mathbf{x}, \mathbf{x}) + k(\mathbf{y}, \mathbf{y}) - 2k(\mathbf{x}, \mathbf{y})$ according to the reproducing property of kernel k (Smola et al., 2007). Note that d_k only depends on $|\mathbf{x} - \mathbf{y}|$ if k is stationary.

In the presence of relevant knowledge, the latent mapping \mathbf{h} is subject to \mathcal{D}_R , which leads to the nonlinear multi-fidelity (NARGP) deep kernel (Perdikaris et al., 2017) in which the input is mapped via the posterior mean μ from $p(\mathbf{h}|\mathcal{D}_R)$ and the distance dependence becomes $d_{\mu}(\mathbf{x}, \mathbf{y}) = |\mu(\mathbf{x}) - \mu(\mathbf{y})|^2$. The lack of uncertainty associated with estimating the hidden mapping may result in unjustified confidence when predicting target function.

The DMM kernel shares properties with the above kernels due to the marginalization (Duvenaud et al., 2014) and the presence of relevant knowledge (Perdikaris et al., 2017), and includes novel, desirable properties. First, conditioned on \mathcal{D}_R , the posterior mean also enters the DMM kernel in the form of d_{μ} as NARGP kernel does. However, the associated

uncertainty encoded in posterior distribution $p(\mathbf{h}|\mathcal{D}_R)$ appears in the form of location-dependent length scale function,

$$\mathcal{L}_{\mathbf{x},\mathbf{y}} = \ell^2 + \text{cov}(h_{\mathbf{x}}, h_{\mathbf{x}}) + \text{cov}(h_{\mathbf{y}}, h_{\mathbf{y}}) - 2\text{cov}(h_{\mathbf{x}}, h_{\mathbf{y}}), \quad (1)$$

where the symbol cov represents the posterior covariance. The presence of non-local length scale function \mathcal{L} makes the DMM kernels non-stationary, which enhances its expressive power for capturing local patterns. When \mathcal{D}_R is sufficient for prediction with low uncertainty, \mathcal{L} is dominated by the constant ℓ^2 and the DMM kernel is reduced to the form in NARGP.

Figure 1 illustrates learning the latent function $h = \sin 8\pi x$ from data (upper panel), and a few samples of $f(x, h(x))$ from GP prior with the DMM kernel (bottom panel). Left panels present the case where the noise level in \mathcal{D}_R is low, and the learned relevant function (top) with low uncertainty results in the smooth random target functions (bottom) sampled from the DMM kernel. High-noise data \mathcal{D}_R , shown on the right, cause higher uncertainty regarding learning h , and, surprisingly, the random samples of $f(x, h(x))$ follow the long-length scale behavior of their counterparts on the left, and additional short-length scale variation as signature of the non-local function \mathcal{L} . Such behavior in prior sampling is not seen with typically tuning the hyperparameters of kernel in standard GP.

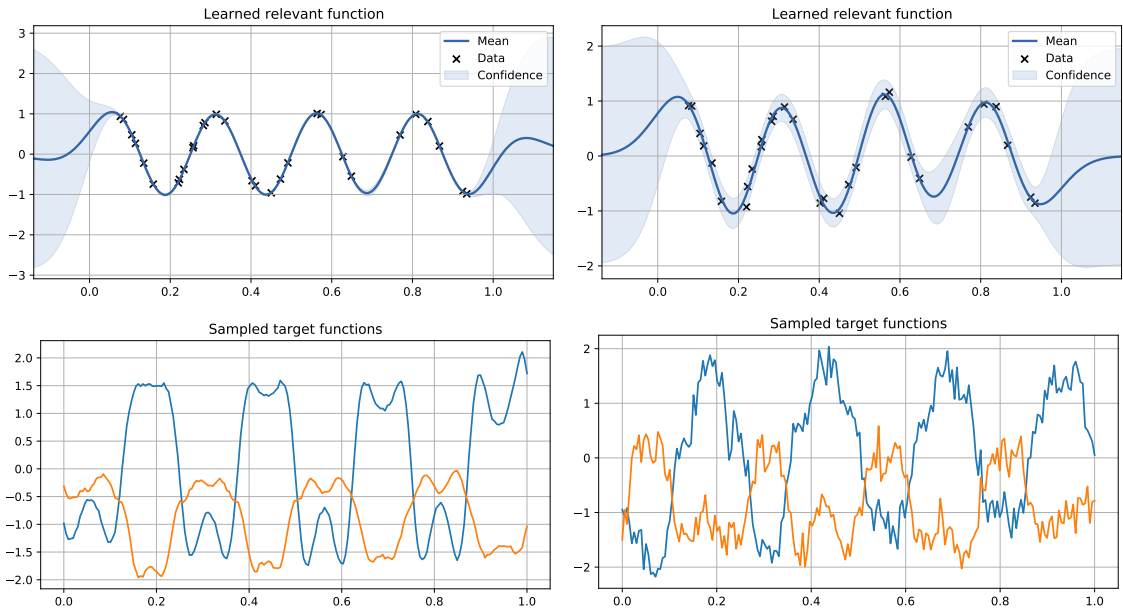


Figure 1: Top row: Reconstruction of relevant function $h(x) = \sin(8\pi x)$ by GP using SE kernel with the relevant data \mathcal{D}_R of noise level $\sigma_n = 0.01$ (left) and $\sigma_n = 0.1$ (right). Bottom row: Random target functions $f(x, h(x))$ sampled from respective DMM kernels with same hyperparameters.

The marginalization over the hidden mapping with the weight of $p(\mathbf{h}|\mathcal{D}_R)$ results in the appearance of squared distance in RKHS in \mathcal{L} . However, in contrast with the DGP kernel d_k , it is the posterior covariance $\text{cov}(h, h)$ in Eq. (1) which appears in \mathcal{L} . The posterior covariance defines the RKHS for the function h subject to the observations in \mathcal{D}_R . In addition, unlike d_k , this squared distance is non-stationary and depends on both $\mathbf{x} + \mathbf{y}$ and $\mathbf{x} - \mathbf{y}$.

1.2 Related Works

Moment matching: Girard et al. (2003) considered the GP regression with uncertain input, and replaced the non-Gaussian predictive distribution with Gaussian one of matched mean and variance. Expectation Propagation in Minka (2001) computed the vector of mean and variance parameters of non-Gaussian posterior distributions. Titsias and Lawrence (2010) approximated the distribution over the unseen pixels as multivariate Gaussian with matched mean and covariance. Moment matching is also popular in comparing two distributions (Muandet et al., 2012) where the embedded means in RKHS are computed. In generative models, the model parameters are learned from comparing the model and data distributions (Li et al., 2015).

Deep probabilistic models: Garnelo et al. (2018) proposed Conditional Neural Process as a stochastic process model which incorporates a subset of observations into a data-informed prior for functions. Deep Gaussian Processes (DGPs) constitute one family of models for composition functions by conditioning input to GP on output of another

GP (Damianou and Lawrence, 2013). Earlier works of warped GP enhanced the expressivity of GP by sending it to another nonlinear mapping (Snelson et al., 2004; Lázaro-Gredilla, 2012). Variational DGP inference exploits the simplicity of approximate Gaussian posterior distribution, and the mean and variance parameters are optimized through ELBO (Salimbeni and Deisenroth, 2017) or EP (Bui et al., 2016). However, the multi-modalness of DGP posterior (Havasi et al., 2018; Lu et al., 2020) may arise from the fact that the hidden mappings in intermediate layers are dependent (Ustyuzhaninov et al., 2020). Inference schemes capable of capturing the multi-modal nature of DGP posterior was recently proposed by Yu et al. (2019).

Multi-source GP regression: Assuming autoregressive relations between data of different fidelity, Kennedy and O’Hagan (2000) proposed a co-kriging model for multi-fidelity regression task. Le Gratiet and Garnier (2014) improved the computational efficiency with a recursive multi-fidelity model. Raissi and Karniadakis (2016) mapped the input space to the latent space and followed the work in Kennedy and O’Hagan (2000). Perdikaris et al. (2017) stacked a sequence of GPs in which the posterior mean about the low-fidelity function is passed to the input of the next GP while the associated uncertainty is neglected. Cutajar et al. (2019a) exploited the DGP structure for the multi-fidelity regression tasks and used the approximate variational inference in (Salimbeni and Deisenroth, 2017). Multi-output GPs (Alvarez et al., 2011; Kaiser et al., 2018; Bruinsma et al., 2019) regard the observations from different data sets as realization of vector-valued function and the corresponding covariance is assumed to have Kronecker product structure.

Kernel composition: Williams (1997) and Cho and Saul (2009) used the basis of error functions and Heaviside polynomial functions to obtain the arc-sine and arc-cosine kernel functions, respectively, of neural networks. Duvenaud et al. (2014) employed the analogy between neural network and GP, and constructed the deep kernel for DGP. Dunlop et al. (2018) analyzed variety of non-stationary kernel compositions in DGP, and Shen et al. (2020) provided an insight from Wigner transformation of general two-input functions. Wilson et al. (2016) proposed the general recipe for constructing the deep kernel with neural networks. Daniely et al. (2016) computed the deep kernel from the perspective of two correlated random variables. Mairal et al. (2014) and Van der Wilk et al. (2017) studied the deep kernels in the convolutional models.

Few-shot and transfer learning: Patacchiola et al. (2019) proposed a GP model with embedding of deep neural network similar to Wilson et al. (2016). With the hyperparameters of GP and deep neural network jointly learned from a collection of many related data sets of small size, the prediction in target task is based on the posterior distribution obtained using the shared hyperparameters.

2 Deep Gaussian Process

We first briefly review Gaussian Process (GP) (Rasmussen and Williams, 2006). GP is the continuum generalization of multivariate Gaussian distribution over a finite set of random variables $\mathbf{f} := \{f_i\}_{i=1:N}$. As the joint distribution over N function values $p(\mathbf{f}) = \mathcal{N}(\mathbf{v}, K)$ is specified by the mean vector \mathbf{v} and kernel matrix K , the random function can be recognized as GP, $f \sim \mathcal{GP}(\mu(\mathbf{x}), k(\mathbf{x}, \mathbf{x}'))$ where the mean function $\mu(\cdot)$ and kernel function $k(\cdot, \cdot)$ are the continuum representative of \mathbf{v} and \mathbf{K} , respectively. GP regression is non-parametric Bayesian as it formulates prediction with the conditional distribution and marginalization,

$$p(y_*|\mathbf{y}) = \int d\mathbf{f} df_* p(y_*|f_*)p(f_*|\mathbf{f})p(\mathbf{f}|\mathbf{y}). \quad (2)$$

The essence of GP prediction is the covariance among the random variables \mathbf{f} and f_* . Selection of covariance function(s) is usually by domain experts. Assuming zero-mean $\mu = 0$ and Gaussian likelihood, the conditional distribution has the analytic form, $p(y_*|\mathbf{y}) = \mathcal{N}(\mu_*, \sigma_*^2)$, along with the following predictive mean and variance,

$$\mu_* = \mathbf{k}(\mathbf{x}_*, \mathbf{X})(K + \sigma_n^2 I_N)^{-1} \mathbf{y}, \quad (3)$$

and

$$\sigma_*^2 = k(\mathbf{x}_*, \mathbf{x}_*) - \mathbf{k}(\mathbf{x}_*, \mathbf{X})K^{-1}(\mathbf{X}, \mathbf{X})\mathbf{k}(\mathbf{X}, \mathbf{x}_*). \quad (4)$$

The hyper-parameters in kernel k are determined by optimizing the marginal likelihood $p(\mathbf{y})$ for the training observations. The kernel function k is key to the properties of random function f . SE kernel $k(\mathbf{x}, \mathbf{x}') \propto \exp(-|\mathbf{x} - \mathbf{x}'|^2/2\ell^2)$ is a common choice for smooth functions whereas the non-stationary Brownian motion kernel can generate stochastic non-differentiable continuous functions.

2.1 DGP joint, posterior, and marginal distributions

Deep Gaussian Process (DGP) has a nested and multi-layered structure of GPs in which GPs in intermediate layers condition their input on the output of the preceding GPs (Damianou and Lawrence, 2013). For regression tasks, the

input to the first GP is fixed while the output of last GP is connected with the observations. In a S -layer DGP, we may label the last GP by the function vector \mathbf{f} while those of intermediate GPs by the latent functions, $\mathbf{h}_{1:S-1}$. The intractability is understood by observing the *DGP joint distribution*,

$$p(\mathbf{f}, \mathbf{h}_{1:S-1} | \mathbf{X}) = p(\mathbf{f} | \mathbf{h}_{S-1}) \cdots p(\mathbf{h}_1 | \mathbf{X}), \quad (5)$$

in which the conditional distributions are Gaussian. The latent functions appear in the exponential quadratic form in $p(\mathbf{h}_i | \mathbf{h}_{i-1})$, and also in the inverse of covariance matrix in $p(\mathbf{h}_{i+1} | \mathbf{h}_i)$ or $p(\mathbf{f} | \mathbf{h}_i)$.

When considering the observations \mathbf{y} as a realization of the output function \mathbf{f} , we may write down the *DGP posterior distribution* as,

$$p(\mathbf{f}, \mathbf{h}_{1:S-1} | \mathbf{y}) = \frac{p(\mathbf{y} | \mathbf{f}) p(\mathbf{f}, \mathbf{h}_{1:S-1})}{p(\mathbf{y})}, \quad (6)$$

in which the marginal likelihood is given by,

$$\begin{aligned} p(\mathbf{y}) &= \int d\mathbf{f} d\mathbf{h}_{1:S-1} p(\mathbf{y} | \mathbf{f}) p(\mathbf{f}, \mathbf{h}_{1:S-1}), \\ &= \int d\mathbf{f} p(\mathbf{y} | \mathbf{f}) p(\mathbf{f}), \end{aligned} \quad (7)$$

where we have defined the *DGP marginal distribution*,

$$p(\mathbf{f}) = \int d\mathbf{h}_{1:S-1} p(\mathbf{f} | \mathbf{h}_{S-1}) \cdots p(\mathbf{h}_1 | \mathbf{X}). \quad (8)$$

The dependence on data matrix \mathbf{X} above is suppressed to ease the notation. Because the hidden functions h 's are not connected with observations \mathbf{y} , we may rewrite the predictive distribution over $f(\mathbf{x}_*)$ as,

$$p(y_*) = \int d\mathbf{f} d\mathbf{f}_* p(y_* | f_*) \frac{p(\mathbf{y} | f_*, \mathbf{f}) p(f_*, \mathbf{f})}{p(\mathbf{y})}. \quad (9)$$

2.2 DGP with multi-source data

In the multi-source regression where the target data set $\mathcal{D}_T = (\mathbf{X}, \mathbf{y})$ and the relevant data set $\mathcal{D}_R = (\mathbf{X}^{(i)}, \mathbf{y}^{(i)})_{i=1}^{S-1}$ are realization of the target function $y = f(\mathbf{x})$ and the latent function $y = h_{1:S-1}(\mathbf{x})$, respectively, we generalize the DGP marginal distribution as,

$$p(\mathbf{f} | \mathcal{D}_R) = \int d\mathbf{h}_{1:S-1} p(\mathbf{f} | \mathbf{h}_{S-1}) p(\mathbf{h}_{S-1} | \mathbf{y}^{(S-1)}, \mathbf{h}_{S-2}) \cdots p(\mathbf{h}_1 | \mathbf{y}^{(1)}). \quad (10)$$

The conditional distributions in Eq. (10) are still Gaussian, but all except the first one, represent the posterior distribution. It is helpful to contemplate the DGP with only one latent function layer, which is shown in the left panel of Fig. 2. In such case, the introduction of \mathcal{D}_R is to constrain the function h subject to the observations $\mathbf{y}^{(1)} = h(\mathbf{X}^{(1)})$ up to some noise. The multi-source DGP marginal distribution in Eq. (10) can then be used in the prediction stage as in Eq. (9).

3 Deep Moment Matching Kernels

The approximate inference in this paper is based on finding tractable and interpretable distribution $q(f)$ to replace the true DGP marginal distribution $p(f)$ in Eq. (10) and in the prediction stage. In general, the target function f is still a random process (Lawrence and Moore, 2007). If the approximate distribution q represents a GP, then we need to compute the associated mean and covariance functions. In the absence of \mathcal{D}_T , it is reasonable to assume f is a zero-mean GP. The second moment, the covariance of f , must match that of the true process,

$$\mathbb{E}_q[f_i f_j] = \mathbb{E}_p[f_i f_j], \quad (11)$$

and the computation depends on the sequence of kernels used in the conditional GPs in Eq. (10).

For convenience, we extend the notation in (Lu et al., 2020). For instance, SE[NN] stands for the two-layer DGP where the target f is a GP with SE kernel while the latent h comes from the posterior GP with neural network kernel. In the following, we shall focus on the analytic results of two-layer DGPs for the two families of models, SE[] and SC[], where the GP for h can use arbitrary kernel function.

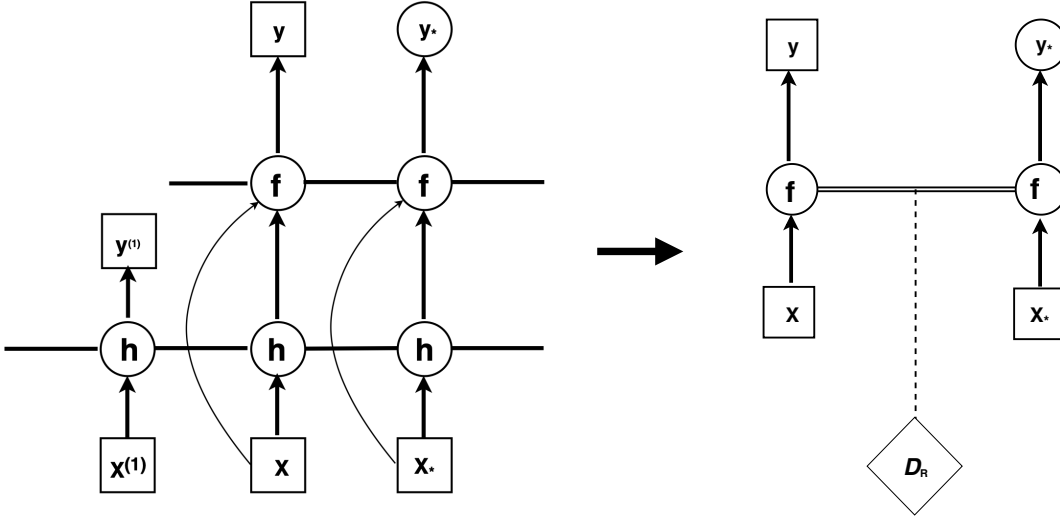


Figure 2: **Left:** Example of 2-source DGP regression model in which the target, $\mathcal{D}_T = \{\mathbf{X}, \mathbf{y}\}$, and the relevant, $\mathcal{D}_R = \{\mathbf{X}^{(1)}, \mathbf{y}^{(1)}\}$, are fused to make prediction for y_* . The function h represents the GP posterior conditioned on \mathcal{D}_R , and the target function f has input in h and \mathbf{x} (illustrated by the curved arrow), and is zero-mean GP. **Right:** the multi-source DGP has the effective GP model with the data-informed DMM kernel.

3.1 Squared Exponential Composition: SE[]

In the case of SE kernel employed in the GP for f , the remark below is useful for computing covariance.

Remark 1. For random continuous function $f \sim \mathcal{GP}(\mu, k)$, the expectation of an exponential quadratic form $\exp[-\frac{1}{2}Q(f_1, f_2, \dots, f_n)]$ with $Q \geq 0$ associated with the n function values $f_{1:n} = f(\mathbf{x}_{1:n})$,

$$\mathbb{E}_{f_{1:n} \sim \mathcal{N}(\mathbf{v}, \mathbf{K})} [e^{-\frac{1}{2}Q(f_{1:n})}] = \frac{\exp[-\frac{1}{2}\mathbf{v}^T \mathbf{K}^{-1}(\mathbf{I}_n - (\mathbf{I}_n + \mathbf{K}\mathbf{A})^{-1})\mathbf{v}]}{\sqrt{|\mathbf{I}_n + \mathbf{K}\mathbf{A}|}} \quad (12)$$

where the vector \mathbf{v} has entries $v_i = \mu(\mathbf{x}_i)$ and the n -by- n matrix $[\mathbf{K}]_{ij} = k(\mathbf{x}_i, \mathbf{x}_j)$ represent the covariance matrix. The symmetric matrix \mathbf{A} is the representation for the quadratic form, i.e. $Q(f_{1:n}) = \sum_{i,j} A_{ij} f_i f_j$.

Thus, the second moment, covariance of f , in DGP marginal distribution is $\mathbb{E}_p[f_i f_j] = \mathbb{E}_{\mathcal{N}}[\sigma^2 e^{-\frac{1}{2}Q(h_i, h_j)}]$ with the representation $\mathbf{A} = \frac{1}{\ell^2} \begin{pmatrix} 1 & -1 \\ -1 & 1 \end{pmatrix}$. σ and ℓ are hyperparameters of SE kernel in GP for f . The posterior over $h_{i,j}$ given \mathcal{D}_R is a bivariate Gaussian with $\mathbf{v} = \begin{pmatrix} \mu_i \\ \mu_j \end{pmatrix}$ and $\mathbf{K} = \begin{pmatrix} k_{ii} & k_{ij} \\ k_{ji} & k_{jj} \end{pmatrix}$. One only needs to compute the inverse of 2×2 matrices to obtain the analytic covariance. The kurtosis, the fourth order moments, can be computed by inverting corresponding 4×4 matrices, which may shed light on the non-Gaussian aspect of Eq. (10).

Lemma 1. The covariance of f in the 2-source DGP marginal distribution in Eq. (10) with SE[] composition is,

$$\mathbb{E}_p[f_i f_j] = \frac{\ell \sigma^2}{\sqrt{\mathcal{L}_{ij}}} \exp\left[-\frac{(\mu_i - \mu_j)^2}{2\mathcal{L}_{ij}}\right] \quad (13)$$

where the non-local parameter $\mathcal{L}_{ij} = \ell^2 + k_{ii} + k_{jj} - 2k_{ij}$ is function of posterior covariance $k_{ij} = \text{cov}(h_i, h_j)$.

The key to prove the above lemma is the matrix identity, $\mathbf{I}_2 - (\mathbf{I}_2 + \mathbf{K}\mathbf{A})^{-1} = \frac{\mathbf{K}\mathbf{A}}{\mathcal{L}_{ij}}$ with which one can show the exponent is $-(\mu_i - \mu_j)^2 / 2\mathcal{L}_{ij}$.

The second moment captures the exact covariance of f in the DGP marginal distribution. Unlike the discussions in Lu et al. (2020) where the conditional GPs in latent layers are zero-mean, the relevant knowledge from learning \mathcal{D}_R

Algorithm 1 DMM Multi-source GP learning

Input: S sources of data: target data $\mathcal{D}_T = (\mathbf{X}, \mathbf{y})$ and relevant data $\mathcal{D}_S = (\mathbf{X}^{(i)}, \mathbf{y}^{(i)})_{i=1}^{S-1}$, kernel functions k for the first GP, and the test input \mathbf{x}_* .

for $i = 1$ to $S - 1$ **do**

1. If $i = 1$; kernel $\leftarrow k$, else: kernel \leftarrow DMM kernel in Eq. (15).
2. GP learning of hyperparameters, σ and ℓ , by optimizing the marginal likelihood of $(\mathbf{X}^{(i)}, \mathbf{y}^{(i)})$.
3. Evaluate the posterior mean and posterior covariance at these inputs, $\mathbf{X}^{(i+1)} \cup \dots \cup \mathbf{X} \cup \mathbf{x}_*$.
4. Compute the DMM kernel for the next GP using Eq. (13) or (14).

end for

GP learning of \mathcal{D}_T with the DMM kernel.

Output: Predictive mean μ_* and variance σ_* at input \mathbf{x}_* .

provides the kernel in Eq. (13) both the confident information by $\mu_i - \mu_j$ and the uncertainty in \mathcal{L} . This is a novel method of data-driven composition of deep multi-scale kernels. The non-local factor \mathcal{L} makes the DMM kernel non-stationary, and the uncertainty in estimating latent function forces the target functions to possess additional short-length scale variation, which can be seen in Fig. 1. Another novelty is that DMM kernel allows the relevant observations to enter the covariance function and the ensuing predictive covariance. Standard GPs do not have the capacity of providing observation-dependent predictive covariance (Shah et al., 2014).

3.2 Squared Cosine Composition: SC[]

Now consider the case where the zero-mean GP for target function f in Figure 2 employs the squared cosine kernel function, i.e. $k(h_i, h_j) = \sigma_2^2 \cos^2 \frac{h_i - h_j}{2\ell_2}$. After rewriting $k(h_i, h_j) = \{2 + \exp[i(h_i - h_j)] + \exp[-i(h_i - h_j)]\}/4$, the same trick can be applied to obtain the covariance of f in the 2-layer DGP marginal distribution Eq. (10).

Lemma 2. *The covariance of target function f of DGP with SC[] composition is,*

$$\mathbb{E}[f_i f_j] = \frac{\sigma_2^2}{2} [1 + \cos(\mu_i - \mu_j) \exp(V_{ij})] \quad (14)$$

where $V_{ij} = (2k_{ij} - k_{ii} - k_{jj})/2\ell_2^2$ represents the posterior covariance from the GP for h .

The proof to above lemma follows from the expectation of exponential function, $\int dh_i h_j e^{(h_i - h_j)\mathbf{a}} \mathcal{N}\left(\begin{smallmatrix} h_i \\ h_j \end{smallmatrix} \middle| \mathbf{v}, \mathbf{K}\right) = \exp(\mathbf{a}^T \mathbf{v} + \mathbf{a}^T \mathbf{K} \mathbf{a} / 2)$, along with the identification of 2×1 vector, $\mathbf{a} = \pm(i, -i)^T$, in the squared cosine composition.

3.3 Implementation

The previous derivations show computations of covariance of target function f in the posterior-prior stacking DGP, SE[] in Eq. (13) and SC[] in Eq. (14). The kernel functions depend on the input \mathbf{x} 's implicitly through the posterior mean $\mu_{i,j}$ and posterior covariance $k_{i,j}$ given the relevant data \mathcal{D}_R . In the implementation, we include the explicit dependence (see Fig. 2) by multiplying the DMM kernels with SE kernel,

$$k_{\text{path}}(\mathbf{x}_i, \mathbf{x}_j) = \sigma^2 \exp\left(\frac{-|\mathbf{x}_i - \mathbf{x}_j|^2}{2\ell^2}\right) k_{\text{DMM}}(\mathbf{x}_i, \mathbf{x}_j), \quad (15)$$

to increase the representational capacity of the model (Duvenaud et al., 2014).

Now we shall apply GP with DMM kernels to the multi-source regression tasks in which the relevant data and their order are indeed helpful to the target domain. Algorithm 1 lists the summary of computations for the DMM kernels in GP multi-source learning. With the S sources of data, the multi-source regression model is built on the S -layer DGP structure. In addition, the kernel function k in the first GP is arbitrary, and the marginal likelihood for $(\mathbf{X}^{(1)}, \mathbf{y}^{(1)})$ is optimized for learning the associated hyperparameters. Then, the posterior mean and posterior covariance evaluated at these inputs, $\mathbf{X}^{(2)} \cup \dots \cup \mathbf{X}^{(S-1)} \cup \mathbf{X} \cup \mathbf{x}_*$, are sent into the DMM kernel in Eq. (13) or (14), depending on the composition, for the subsequent GP learning of the second source in \mathcal{D}_R , i.e. $(\mathbf{X}^{(2)}, \mathbf{y}^{(2)})$. Continuing the procedure until the learning of $(\mathbf{X}^{(S-1)}, \mathbf{y}^{(S-1)})$ is done, we shall obtain the DMM kernel for the final GP learning on the data \mathcal{D}_T and the subsequent prediction on $f(\mathbf{x}_*)$. The inference time complexity for the present model is proportional to $|\mathbf{X}|^3 + \sum_i |\mathbf{X}_i|^3$.

4 Experiments

Using GPy (GPy, 2012) as backbone, the standard procedure of GP hyper-parameter learning is followed and the two families of DMM kernels (SE[] and SC[]) along with the gradients in the space of $\{\sigma, \ell\}$ are implemented.¹ We demonstrate the effectiveness of DMM kernels by simulating on three kinds of multi-source data: 1) synthetic nonlinear function regression where the target function $f(x) = f(x, h(x))$ is a composite function and the observations in the two sources, \mathcal{D}_T and \mathcal{D}_R , are realization of $y = f(x)$ and $y = h(x)$, respectively. 2) synthetic denoising regression about the target function $y = f(x)$ given the rare and noiseless observations in \mathcal{D}_T and plentiful but noisy ones in \mathcal{D}_R . 3) real-world multi-fidelity data regression in Cutajar et al. (2019a) where the input space \mathbf{x} is of high dimension and the relevant data source \mathcal{D}_R may contain multiple data sets. The public code source in Cutajar et al. (2019b) provides the implementation of AR1 (Kennedy and O’Hagan, 2000), NARGP (Perdikaris et al., 2017), DEEP-MF (Raissi and Karniadakis, 2016), and MF-DGP (Cutajar et al., 2019a). The Linear Coregionalized regression model (LCM) (Alvarez et al., 2011) implementation is available from (Andrade-Pacheco, 2015).

4.1 Synthetic two-fidelity function regression

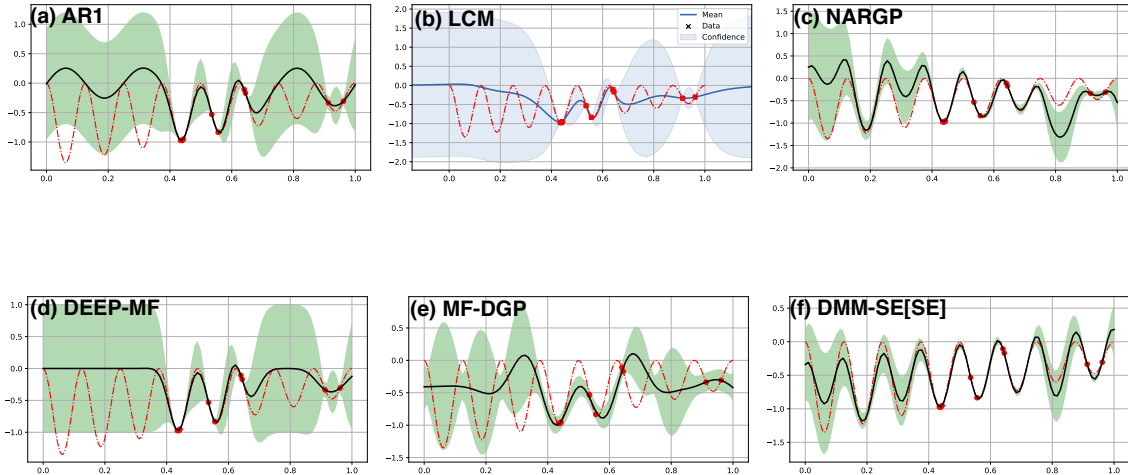


Figure 3: Multi-fidelity regression on relevant function, $h(x) = \sin 8\pi x$, with 30 observations (not shown) and target function, $f(x) = (x - \sqrt{2})h^2(x)$ (dashed line), with 10 observations (red dots). Only the target prediction (solid) and associated uncertainty (shaded) are shown: top row: (a) AR1, (b) LCM, (c) NARGP. bottom row: (d) DEEP-MF, (e) MF-DGP, (f) DMM-SE[SE].

The first example in Figure 3 consists of 10 random observations of the target function $f(x) = (x - \sqrt{2})h^2(x)$ (red dashed line) along with 30 observations of the relevant function $h(x) = \sin 8\pi x$ (not shown). The 30 observations of h with a period 0.25 in the range of $[0, 1]$ is more than sufficient to reconstruct the relevant function h with high confidence. In contrast, the 10 observations of f (shown in red dots) are difficult to reconstruct the true f if GP with SE kernel is used. The above figures demonstrates the results from a set of multi-source nonparametric regression methods which incorporate the learning of h into the target regression of f . The DMM SE[SE] [panel (f)] kernel and NARGP [panel (c)] successfully capture the periodic pattern inherited from the relevant function h , but the target function is fully covered in the confidence region in the prediction of DMM SE[SE] only. On the other hand, in the input space away from the target observations, AR1 [panel (a)] and MF-DGP [panel (e)] manages to only capture part of the oscillation. Predictions in LCM [panel (b)] and DEEP-MF [panel (d)] are reasonable near the target observations but fail to capture the oscillation away from these observations.

Figure 4 demonstrates another example of multi-fidelity regression on the nonlinear composite function. The relevant function is also periodic, $h = \cos 15x$, and the target is exponential function of the relevant one, $f = x \exp[h(2x-2)] - 1$. The 15 observations of f (red dashed line) are marked by the red dots. The exponential nature in the mapping $h \mapsto f$

¹github.com/luck1226/multisource_deepGaussianProcess

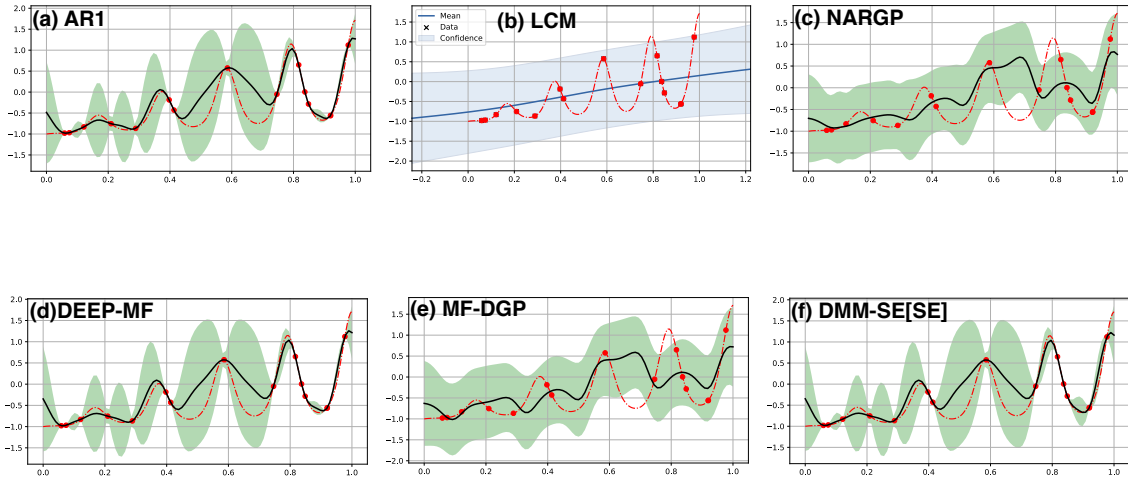


Figure 4: Multi-fidelity regression on the low-level true function, $h(x) = \cos 15x$, with 30 observations and high-level one, $f(x) = x \exp[h(2x - 0.2)] - 1$, with 15 observations. (top row: (a) AR1, (b) LCM, and (c) NARGP. bottom row: (d) DEEP-MF, (e) MF-DGP, and (f) DMM-SE[SE])

might make the reconstruction more challenging than the previous case, which may lead to less satisfying result from LCM [panel (b)]. NARGP [panel (c)] and MF-DGP [panel (e)] have similar predictions which mismatch some of the observations, but the target function is mostly covered by the uncertainty estimation. The DMM-SE[SE] kernel [panel (f)], on the other hand, has predictions consistent with all the target observations, and the target function is fully covered by the uncertainty region. Qualitatively similar results are also obtained from AR1 [panel (a)] and DEEP-MF [panel (d)].

4.2 Denoising regression

Here we consider the denoising regression task in which there are two data sets realizing the target function $f(x) = (x - \sqrt{2}) \sin^2 8\pi x$ (red dashed line in Figure 5). The data set \mathcal{D}_T contains 15 observations of f with noise level of 0.001 (red dots) while the second data set \mathcal{D}_R consists of 30 observations of the same function but with noise level of 0.1 (dark cross symbol). Now we treat \mathcal{D}_R as observations of some unknown but relevant function h , and the true target function has the relation $f = f(x, h(x))$. Unlike the previous regression tasks where the target function f has a fixed relation with the relevant function h , the data of different noise level can not be mapped into each other with a predetermined transformation. However, given \mathcal{D}_R , the structure of DGP allows the posterior over h to emit infinitely many samples of h into the GP regression models for the target function f . Qualitatively, one can expect that the actual prediction for f is the average over the GP models with different information of h . Consequently, we may expect the variance obtained from the present method to be reduced.

Indeed, as shown in Figure 5, the variance predicted using single GP with the high-noise observations in \mathcal{D}_R is marked by the light-blue region around the predictive mean (light-blue solid line). However, when the prediction encoded in the posterior $p(h|\mathcal{D}_R)$ is transferred to the DMM-SE[SE] kernel, the new GP with this data-informed kernel is shown to possess much tighter uncertainty (marked by the light-green shaded region) around the improved predictive mean (dark solid line) even in the region away from the low-noise observations.

4.3 Real-world multi-fidelity regression

The work in (Cutajar et al., 2019a) along with the code in (Cutajar et al., 2019b) assembles a set of multi-fidelity regression data sets in which the input \mathbf{x} is of high dimension and the levels of fidelity may be more than 2, i.e. there may be multiple sources of data in \mathcal{D}_R . The simulation is performed using the DMM SE[SE] and SC[SE] kernels for the two-fidelity regression data sets (Currin, Park, and Borehole). For the three-fidelity regression data sets (Branin and Hartmann3D), the DMM SE[SE[SE]] and SC[SC[SE]] kernels are employed. The performance of generalization is measured in terms of RMSE and mean negative log likelihood (MNLL). Table 2 displays the results from the

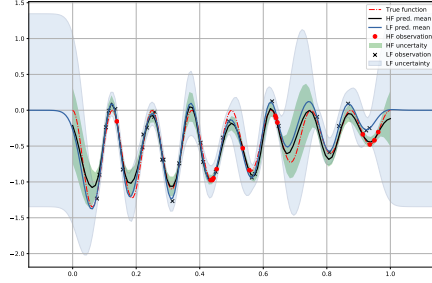


Figure 5: Denoising regression with 30 high-noise (\mathcal{D}_R cross symbol) and 15 low-noise (\mathcal{D}_T red circle) observations from the function $y = (x - \sqrt{2}) \sin^2 8\pi x$ (red dashed line). The uncertainty is reduced in the GP learning with DMM kernels.

AR1 (Cutajar et al., 2019b), MF-DGP (Cutajar et al., 2019b), DMM SE[] and DMM SC[]. We also include the simulation of GP regression with only the target data set \mathcal{D}_T .

Table 2: Results (RMSE, MNLL) of multi-fidelity regression

	AR1	MF-DGP	DMM-SE[]	DMM-SC[]	GP(on \mathcal{D}_T)
Currin	(0.76, 205)	(0.61, 1.05)	(0.67, 3.42)	(0.66, 3.07)	(0.68, 3.29)
Park	(0.60, 328)	(0.54, 1.25)	(0.92, 22.9)	(0.95, 25.0)	(1.69, 1.86)
Borehole	(0.004, -3.94)	(0.015, -1.87)	(0.034, -2.08)	(0.034, -2.08)	(0.39, 0.56)
Branin	(0.01, -3.7)	(0.01, -2.7)	(0.03, -2.9)	(0.03, -2.9)	(0.91, 5180)
Hartmann3D	(0.04, -1.8)	(0.095, -0.77)	(0.18, -0.4)	(0.16, -0.3)	(0.44, 0.68)

We may summarize the performance of the GP with DMM kernels from two categories of data sets. The first category consists of Currin ($|\mathcal{D}_{T,R}| = 5, 12$) and Park ($|\mathcal{D}_{T,R}| = 5, 30$) data sets with which the standard GP regression, with high-level observations only (last column), outperforms AR1 in terms of MNLL. In this category, while the number of observations is low, MF-DGP, augmented by the optimized inducing points, has the most superior results in both RMSE and MNLL. The GP with DMM SC[SE] has the second best MNLL for the Currin data set. The second category, on the other hand, made up of the rest data sets, have sufficient relevant observations. In addition, the opposite trend is shown, i.e. the usage of standard GP with the highest-level observations only results in the poorest performance. Moreover, AR1 has the better results than MF-DGP and DMM kernels. We note that, for Branin data set, both the DMM kernels outperform MF-DGP in terms of MNLL.

5 Conclusion

We investigate the multi-source DGP by computing the covariance, the second moment, of the target function in the DGP marginal distribution, and approximate the DGP with GP and the deep moment matching kernels. The knowledge about the latent functions learned from the relevant data sets is represented in the form of kernel function which also includes the uncertainty information. The DMM kernels for the target functional space are non-stationary as the posterior covariance from inferring the latent functions is enclosed in the non-local length scale function. Sampled functions from such data-informed kernels show distinct behaviors not seen by simply tuning the hyperparameters. In addition, the approximation of a complex stochastic process with a GP using the DMM kernels is effective in the regression tasks where the number of target observations is few but there are plentiful observations made from relevant sources.

References

- Alvarez, M. A., Rosasco, L., and Lawrence, N. D. (2011). Kernels for vector-valued functions: A review. *arXiv preprint arXiv:1106.6251*.
- Andrade-Pacheco, R. (2015). Coregionalized regression tutorial. https://github.com/SheffieldML/notebook/blob/master/GPy/coregionalized_regression_tutorial.ipynb.

- Bruinsma, W. P., Perim, E., Tebbutt, W., Hosking, J. S., Solin, A., and Turner, R. E. (2019). Scalable exact inference in multi-output gaussian processes. *arXiv preprint arXiv:1911.06287*.
- Bui, T., Hernández-Lobato, D., Hernandez-Lobato, J., Li, Y., and Turner, R. (2016). Deep gaussian processes for regression using approximate expectation propagation. In *International Conference on Machine Learning*, pages 1472–1481.
- Cho, Y. and Saul, L. K. (2009). Kernel methods for deep learning. In *Advances in neural information processing systems*, pages 342–350.
- Cutajar, K., Pullin, M., Damianou, A., Lawrence, N., and González, J. (2019a). Deep gaussian processes for multi-fidelity modeling. In *Third Bayesian Deep Learning Workshop, Advances in Neural Information Processing Systems, NeurIPS 2018, Montreal (arXiv:1903.07320)*.
- Cutajar, K., Pullin, M., Damianou, A., Lawrence, N., and González, J. (2019b). emukit/mfdgp. https://github.com/amzn/emukit/tree/master/emukit/examples/multi_fidelity_dgp.
- Damianou, A. and Lawrence, N. (2013). Deep gaussian processes. In *Artificial Intelligence and Statistics*, pages 207–215.
- Daniely, A., Frostig, R., and Singer, Y. (2016). Toward deeper understanding of neural networks: The power of initialization and a dual view on expressivity. In *NIPS*.
- Dunlop, M. M., Girolami, M. A., Stuart, A. M., and Teckentrup, A. L. (2018). How deep are deep gaussian processes? *The Journal of Machine Learning Research*, 19(1):2100–2145.
- Duvenaud, D., Rippel, O., Adams, R., and Ghahramani, Z. (2014). Avoiding pathologies in very deep networks. In *Artificial Intelligence and Statistics*, pages 202–210.
- Garnelo, M., Rosenbaum, D., Maddison, C., Ramalho, T., Saxton, D., Shanahan, M., Teh, Y. W., Rezende, D., and Eslami, S. A. (2018). Conditional neural processes. In *International Conference on Machine Learning*, pages 1704–1713.
- Girard, A., Rasmussen, C. E., Candela, J. Q., and Murray-Smith, R. (2003). Gaussian process priors with uncertain inputs application to multiple-step ahead time series forecasting. In *Advances in neural information processing systems*, pages 545–552.
- GPy (since 2012). GPy: A gaussian process framework in python. <http://github.com/SheffieldML/GPy>.
- Havasi, M., Hernández-Lobato, J. M., and Murillo-Fuentes, J. J. (2018). Inference in deep gaussian processes using stochastic gradient hamiltonian monte carlo. In *Advances in Neural Information Processing Systems*, pages 7506–7516.
- Kaiser, M., Otte, C., Runkler, T., and Ek, C. H. (2018). Bayesian alignments of warped multi-output gaussian processes. In *Advances in Neural Information Processing Systems*, pages 6995–7004.
- Kennedy, M. C. and O’Hagan, A. (2000). Predicting the output from a complex computer code when fast approximations are available. *Biometrika*, 87(1):1–13.
- Lawrence, N. D. and Moore, A. J. (2007). Hierarchical gaussian process latent variable models. In *Proceedings of the 24th international conference on Machine learning*, pages 481–488.
- Lázaro-Gredilla, M. (2012). Bayesian warped gaussian processes. In *Advances in Neural Information Processing Systems*, pages 1619–1627.
- Le Gratiet, L. and Garnier, J. (2014). Recursive co-kriging model for design of computer experiments with multiple levels of fidelity. *International Journal for Uncertainty Quantification*, 4(5).
- Li, Y., Swersky, K., and Zemel, R. (2015). Generative moment matching networks. In *International Conference on Machine Learning*, pages 1718–1727.
- Lu, C.-K., Yang, S. C.-H., Hao, X., and Shafto, P. (2020). Interpretable deep gaussian processes with moments. In *International Conference on Artificial Intelligence and Statistics*, pages 613–623.
- Mairal, J., Koniusz, P., Harchaoui, Z., and Schmid, C. (2014). Convolutional kernel networks. In *Advances in neural information processing systems*, pages 2627–2635.
- Minka, T. P. (2001). Expectation propagation for approximate bayesian inference. In *Proceedings of the Seventeenth conference on Uncertainty in artificial intelligence*, pages 362–369. Morgan Kaufmann Publishers Inc.
- Muandet, K., Fukumizu, K., Dinuzzo, F., and Schölkopf, B. (2012). Learning from distributions via support measure machines. In *Advances in neural information processing systems*, pages 10–18.

- Patacchiola, M., Turner, J., Crowley, E. J., O’Boyle, M., and Storkey, A. (2019). Deep kernel transfer in gaussian processes for few-shot learning. *arXiv preprint arXiv:1910.05199*.
- Perdikaris, P., Raissi, M., Damianou, A., Lawrence, N., and Karniadakis, G. E. (2017). Nonlinear information fusion algorithms for data-efficient multi-fidelity modelling. *Proceedings of the Royal Society A: Mathematical, Physical and Engineering Sciences*, 473(2198):20160751.
- Raissi, M. and Karniadakis, G. (2016). Deep multi-fidelity gaussian processes. *arXiv preprint arXiv:1604.07484*.
- Rasmussen, C. E. and Williams, C. K. I. (2006). *Gaussian Process for Machine Learning*. MIT press, Cambridge, MA.
- Salimbeni, H. and Deisenroth, M. (2017). Doubly stochastic variational inference for deep gaussian processes. In *Advances in Neural Information Processing Systems*.
- Schölkopf, B., Smola, A., and Müller, K.-R. (1998). Nonlinear component analysis as a kernel eigenvalue problem. *Neural computation*, 10(5):1299–1319.
- Shah, A., Wilson, A., and Ghahramani, Z. (2014). Student-t processes as alternatives to gaussian processes. In *Artificial intelligence and statistics*, pages 877–885.
- Shen, Z., Heinonen, M., and Kaski, S. (2020). Learning spectrograms with convolutional spectral kernels. In *International Conference on Artificial Intelligence and Statistics*, pages 3826–3836.
- Smola, A., Gretton, A., Song, L., and Schölkopf, B. (2007). A hilbert space embedding for distributions. In *International Conference on Algorithmic Learning Theory*, pages 13–31. Springer.
- Snelson, E., Ghahramani, Z., and Rasmussen, C. E. (2004). Warped gaussian processes. In *Advances in neural information processing systems*, pages 337–344.
- Titsias, M. and Lawrence, N. (2010). Bayesian gaussian process latent variable model. In *Proceedings of the Thirteenth International Conference on Artificial Intelligence and Statistics*, pages 844–851.
- Ustyuzhaninov, I., Kazlauskaitė, I., Kaiser, M., Bodin, E., Campbell, N., and Ek, C. H. (2020). Compositional uncertainty in deep gaussian processes. In *Conference on Uncertainty in Artificial Intelligence*, pages 480–489. PMLR.
- Van der Wilk, M., Rasmussen, C. E., and Hensman, J. (2017). Convolutional gaussian processes. In *Advances in Neural Information Processing Systems*, pages 2849–2858.
- Williams, C. K. (1997). Computing with infinite networks. In *Advances in neural information processing systems*, pages 295–301.
- Wilson, A. G., Hu, Z., Salakhutdinov, R., and Xing, E. P. (2016). Deep kernel learning. In *Artificial Intelligence and Statistics*, pages 370–378.
- Yu, H., Chen, Y., Low, B. K. H., Jaillet, P., and Dai, Z. (2019). Implicit posterior variational inference for deep gaussian processes. In *Advances in Neural Information Processing Systems*, pages 14502–14513.